Leukemia (2016) **30,** 1116–1125

www.nature.com/leu

OPEN

ORIGINAL ARTICLE

Clonal B cells in Waldenström's macroglobulinemia exhibit functional features of chronic active B-cell receptor signaling

KV Argyropoulos[1], R Vogel[2], C Ziegler[2], G Altan-Bonnet[2], E Velardi[1], M Calafiore[1], A Dogan[3], M Arcila[3], M Patel[4], K Knapp[4], C Mallek[4], ZR Hunter[5], SP Treon[5], MRM van den Brink[1,6] and ML Palomba[6]

Waldenström's macroglobulinemia (WM) is a B-cell non-Hodgkin's lymphoma (B-NHL) characterized by immunoglobulin M (IgM) monoclonal gammopathy and the medullary expansion of clonal lymphoplasmacytic cells. Neoplastic transformation has been partially attributed to hyperactive MYD88 signaling, secondary to the MYD88 L265P mutation, occurring in the majority of WM patients. Nevertheless, the presence of chronic active B-cell receptor (BCR) signaling, a feature of multiple IgM+ B-NHL, remains a subject of speculation in WM. Here, we interrogated the BCR signaling capacity of primary WM cells by utilizing multiparametric phosphoflow cytometry and found heightened basal phosphorylation of BCR-related signaling proteins, and augmented phosphoresponses on surface IgM (sIgM) crosslinking, compared with normal B cells. In support of those findings we observed high sIgM expression and loss of phosphatase activity in WM cells, which could both lead to signaling potentiation in clonal cells. Finally, led by the high-signaling heterogeneity among WM samples, we generated patient-specific phosphosignatures, which subclassified patients into a 'high' and a 'healthy-like' signaling group, with the second corresponding to patients with a more indolent clinical phenotype. These findings support the presence of chronic active BCR signaling in WM while providing a link between differential BCR signaling utilization and distinct clinical WM subgroups.

Leukemia (2016) **30,** 1116–1125; doi:10.1038/leu.2016.8

INTRODUCTION

B-cell receptor (BCR) signaling governs cellular homeostasis throughout all stages of mature B-cell differentiation. Naive, antigen-inexperienced cells, which constitute the majority of the mature B-cell pool, require low levels of tonic BCR signaling for their survival,[1] while antigen-induced BCR signaling, in the presence of cytokine and co-receptor signaling, initiates a cascade of B-cell activation, clonal expansion, and subsequent memory and plasma cell formation.[2] The sequence of intracellular events following BCR engagement in normal B cells has been extensively investigated over the last 20 years. Cross-linking of surface immunoglobulins induces tyrosine phosphorylation of the immunoreceptor tyrosine-based activation motifs of Igα and Igβ by Src family kinases (SFK), which recruit and activate the spleen tyrosine kinase (SYK), which in turn mediates the activation of Bruton's tyrosine kinase (BTK), the adapter B-cell linker protein (BLNK), and the phosphatidylinositol-4,5-bisphosphate 3-kinase (PI3K)/ protein kinase B (AKT) axis, among other G-proteins, phosphatases and lipid hydrolases. This cascade of proximal events results in the formation of a multi-protein signaling complex, known as the BCR signalosome, whose ultimate effector is phospholipase C-gamma-2 (PLCγ2), a fundamental molecule for the activation of downstream protein targets, including extracellular-signal-regulated kinase (ERK) and nuclear factor kappa-light-chain-enhancer of activated B cells (NF-κB (Supplementary Figure 1).[3–7] The presence of aberrant BCR signaling has long been established as a key feature of B-cell lymphomagenesis.[8] Specifically, the phenomenon of chronic active BCR signaling has been evidenced by skewed immunoglobulin heavy chain variable region (IGHV) segment usage, BCR upregulation and preclustering, signaling molecule mutations and strong BCR-related transcriptome and phosphorylation signatures.[8,9] Aspects of it have been demonstrated in the context of multiple immunoglobulin M (IgM)+ B-cell non-Hodgkin's lymphoma subtypes, yet more consistently in activated B-cell like diffuse large B-cell lymphoma[10,11] and chronic lymphocytic leukemia (CLL).[12,13]

Waldenström's macroglobulinemia (WM) is an indolent B-cell non-Hodgkin's lymphoma characterized by the accumulation of IgM-secreting clonal lymphoplasmacytic cells in the bone marrow and extramedullary sites.[14] After an extensive characterization of the genomic landscape in WM, MYD88 L265P (>90% of cases) and CXCR4-WHIM (warts, hypogammaglobulinemia, Infections, myelokathexis)-like mutations (~27% of cases) have emerged as the pathologic hallmarks of the disease, demonstrating the significance of these two signaling axes in the pathobiology of WM.[15–17] BCR-signaling-associated mutations occur less frequently, and are restricted to the CD79A and CD79B genes, in approximately 15% of WM cases.[16,18] The strongest evidence for BCR utilization in WM, stems from IGHV studies, which demonstrate a high mutational load and skewed repertoire, suggesting past *in vivo* activation of the pathway.[19–21] SYK and BTK inhibition have been shown to have tumoricidal effects in pre-clinical studies focused on WM cell lines,[22,23] while targeting BTK with ibrutinib in the recently completed clinical trial NCT0161482 generated overall

[1]Immunology Program, Memorial Sloan Kettering Cancer Center, New York, NY, USA; [2]Computational Biology Program, Memorial Sloan Kettering Cancer Center, New York, NY, USA; [3]Department of Pathology, Memorial Sloan Kettering Cancer Center, New York, NY, USA; [4]Hematologic Oncology Tissue Bank, Memorial Sloan Kettering Cancer Center, New York, NY, USA; [5]Bing Center for Waldenström's Macroglobulinemia, Dana Farber Cancer Institute, Boston, MA, USA and [6]Lymphoma Service, Department of Medicine, Memorial Sloan Kettering Cancer Center, New York, NY, USA. Correspondence: Dr ML Palomba, Lymphoma Service, Department of Medicine, Memorial Sloan Kettering Cancer Center, 1275 York Ave, New York, NY 10065, USA.
E-mail: Palombam@mskcc.org
Received 10 July 2015; revised 23 November 2015; accepted 22 December 2015; accepted article preview online 12 February 2016; advance online publication, 4 March 2016

response rates of 90.5% among refractory/relapsed patients.[24] Nevertheless, considering that both SYK and BTK are elements of multiple signaling pathways, including toll-like receptors (TLR), chemokine receptors, integrins and Fc receptors, the role of BCR signaling and its net contribution in WM remains ill-defined.

To comprehend the activity of the BCR network in primary WM cells, we interrogated multiple BCR-related phosphoproteins in a resting and *ex vivo* stimulated state, utilizing multiparametric phosphoflow cytometry, which allows the precise quantification of multiple signaling events at a single-cell level.[25,26] We evaluated aspects of network remodeling in WM cells, compared with physiological BCR signaling, examined the potency of *in vitro* and *in vivo* proximal kinase inhibition, and evaluated upregulated presentation of surface IgM (sIgM) and decreased phosphatase activity as key elements that shape aberrant BCR signaling. Moreover, by using patient-specific phosphosignatures we were able to identify distinct subgroups with clinical significance, elucidating the dependence of different disease states on BCR utilization.

METHODS

Patients and sample processing

We utilized primary samples from 32 WM patients who had previously signed informed consent to have their sample used for research purposes, in accordance with the Declaration of Helsinki and approval by the Memorial Sloan Kettering Cancer Center, Institutional Review Board. The clinical characteristics of all patients are described in Table 1. Matched pre- and post-treatment samples from eight patients enrolled in the clinical trial NCT01614821 for ibrutinib in WM (clinicaltrials.gov) were utilized, and their response characteristics are summarized on Table 2. All eight patients carried the MYD88 L265P mutation, whereas four of them additionally carried CXCR4-WHIM-like S338X mutations, as assessed by allele-specific polymerase chain reaction, for the purposes of the clinical trial. Mononuclear cells were isolated from WM bone marrows and in three cases from a lymph node, pleural fluid and peripheral blood with significant clonal involvement. As a control mononuclear cells were obtained from the peripheral blood and bone marrow of healthy donors (HDs). Mononuclear cells isolation was performed using density gradient centrifugation (Ficoll-Paque Plus; GE Healthcare, Pittsburgh, PA, USA) and cryopreserved in freezing medium (90% fetal bovine serum and 10% dimethyl sulfoxide) in liquid nitrogen. For all signaling experiments, mononuclear cells were thawed and washed in pre-warmed complete medium (Roswell Park memorial Institute, 10% fetal bovine serum, 2% L-glutamine, 1% penicilin–

Table 2. Characteristics of eight WM patients on active ibrutinib treatment

Patient code	*Response*	*Change in serum IgM (%)*	*Change in IT clonal infiltration (%)*	*MYD88 status*	*CXCR4 status*
WM2	VGPR	−89	−40	MUT	WT
WM3	PR	−62	−100	MUT	MUT
WM5	PR	−81	−61	MUT	WT
WM6	PR	−55	−71	MUT	MUT
WM7	PR	−63	125	MUT	MUT
WM10	PR	−71	−12.50	MUT	WT
WM12	PD	77	14	MUT	WT
WM13	SD	−19	−45	MUT	MUT

Abbreviations: IgM, immunoglobulin; IT, intratrabecular; MUT, mutated; PR, partial response; SD, stable disease; VGPR, very good partial response; WM, Waldenström's macroglobulinemia; WT, wild type.

Table 1. Patient characteristics

	Sex	*Light chain*	*Sample tissue*	*Prior-MGUS*	*Status on sample date*
WM2	F	κ	LN	Y	Progressive disease
WM3	M	κ	BM	N	Progressive disease
WM4	F	κ	BM	N	Progressive disease
WM5	F	κ	BM	N	Progressive disease
WM6	M	κ	BM	N	Progressive disease
WM7	M	λ	BM	N	Progressive disease
WM9	F	κ	BM	Y	Stable disease—observation
WM10	M	κ	BM	N	Progressive disease
WM11	M	κ	BM	N	Progressive disease
WM12	M	λ	BM	N	Progressive disease
WM13	M	κ	BM	N	Stable disease—observation
WM14	F	κ	BM	N	Progressive disease
WM15	M	κ	BM	Y	Stable disease—observation
WM18	M	λ	BM	N	Progressive disease
WM19	F	κ	BM	N	Progressive disease
WM22	F	κ	BM	N	Stable disease—observation
WM23	F	κ	BM	N	Progressive disease
WM24	M	κ	BM	N	Stable disease—observation
WM25	F	κ	BM	N	Progressive disease
WM26	M	κ	BM	N	Stable disease—observation
WM27	F	κ	PF	N	Progressive disease
WM28	F	κ	BM	N	Stable disease—observation
WM29	F	κ	BM	N	Progressive disease
WM31	M	κ	BM	N	Stable disease—observation
WM34	M	κ	BM	N	Stable disease—observation
WM35	M	λ	BM	N	Progressive disease
WM36	M	κ	BM	N	Stable disease—observation
WM40	M	κ	BM	N	Stable disease—observation
WM41	F	λ	BM	N	Stable disease—observation
WM44	M	κ	BM	N	Progressive disease
WM50	M	κ	PB	N	Progressive disease
WM51	M	κ	BM	N	Progressive disease

Abbreviations: BM, bone marrow; F, female; LN, lymph node; M, male; MGUS, monoclonal gammopathy of undetermined significance; N, no; PB, peripheral blood; PF, pleural fluid; Y, yes.

streptomycin). After washing, mononuclear cells were resuspended in concentrations up to 10^7 cells/ml, and allowed to rest at 37 °C for 2 h in complete medium. The resting period of 2 h was chosen on the basis that it allowed enhanced *ex vivo* phosphoresponses, compared with minimally rested cells, as shown by previous human BCR stimulation studies published by our group and others.[27,28]

Stimulation protocol and reagents

After the resting period, mononuclear cells were stained in phosphate-buffered saline (PBS) with a LIVE/DEAD fixable yellow dead cell stain (Life Technologies, Carlsbad, CA, USA) for 30 min, followed by resuspension in complete medium and splitting in a U-bottom 96-well plate. BCR signaling was examined at basal state and after sIgM cross-linking by goat polyclonal anti-IgM F(ab′)$_2$ fragments (Life Technologies) at 37 °C. For maximal phosphorylation induction, sIgM was cross-linked in the presence of 3.3 mM hydrogen peroxide—H_2O_2 (Sigma Aldrich, St Louis, MO, USA), as previously described.[6] Cells were stimulated with 10 μg/ml anti-IgM F(ab′)$_2$ for 4 min while dose-response and time-course experiments were also performed. For *in vitro* signaling inhibition experiments, preinhibition was performed with the small molecules Src inhibitor dasatinib (Cell Signaling Technology), SYK inhibitor tamatinib-R406 (Selleckchem, Houston, TX, USA) and BTK inhibitor ibrutinib-PCI32765 (Selleckchem). After stimulation, signaling propagation was stopped with the addition of pre-warmed paraformaldehyde solution, 4% in PBS (Affymetrix, Santa Clara, CA, USA; USB Corporation). Cells were fixed for 10 min at 37 °C, washed with PBS and subsequently permeabilized with cold methanol at − 20 °C. Samples were stored at − 20 °C until the staining step, for no longer than 48 h. Post permeabilization, cells were washed twice with PBS+0.5% bovine serum albumin and stained anti-surface and anti-phosphoprotein antibodies for 30 min at room temperature. Anti-CD20—PerCP-Cy5.5, clone H1 (BD Biosciences, San Jose, CA, USA), anti-kappa—Alexa Fluor 700, clone G20-193 (BD Biosciences) and anti-lambda—BV421, clone JDC-12 (BD Biosciences) were utilized as surface markers, and clonal WM cells were detected based on CD20 expression and light chain restriction. Patients with no detectable clonal involvement by flow cytometry were excluded from this study. Although the normal counterpart of WM cells is still a subject of speculation, it belongs to a mature IgM+ B-cell, of either post-germinal center or marginal-zone-like origin. HD CD20+ circulating B-cells, which are in their vast majority IgM+ mature cells, served as the best healthy control for the purposes of our study. As an additional control we interrogated normal bone marrow CD20+CD10- mature B-cells and CD138+ plasma cells; CD10—APC, clone HI10a, CD138—Brilliant Violet 711, clone (BD Biosciences). Additional surface markers used included anti-human anti-IgM F(ab′)$_2$—FITC (Invitrogen Biosource, Carlsbad, CA, USA), anti-IgM—Brillian Violet 650 (BD Biosciences), clone MHM-88, anti-CD22—APC, clone S-HCL-1 (BD Biosciences) and anti-CD45—APC-H7, CLONE 2D1 (BD Biosciences). Anti-pSFK/pLCK(Y505)—Alexa Fluor 647, clone 4/LCK-Y505, anti-pSYK(Y348)—PE, clone I120-722, anti-pBTK(Y551)/Itk(Y511)—PE, clone24a/BTK(Y551) anti-pBLNK(Y84)—Alexa Fluor 647, clone J117-1278, anti-pPLCγ2(Y759)—Alexa Fluor 488, clone K86-689.37 and anti-pAKT(S473)—Alexa Fluor 647, clone M89-61, were from BD Biosciences, whereas ppERK1/2(T202/Y204)—Alexa Fluor 488, clone E10, and pNF-κB/p65(S536)—PE, clone 93H1, were from Cell Signaling Technology. SHP-1 and SHIP-1 staining was performed with primary anti-SHP-1, clone C14H6 and anti-SHIP-1, clone C40G9, both from Cell Signaling Technology and subsequent staining with a secondary goat anti-rabbit antibody-Pacific-Blue conjugate (ThermoFisher Scientific, Waltham, MA, USA). For total protein staining we fixed and permeabilized mononuclear cells as described for phosphoflow experiments. We utilized the preconjugated antibodies: anti-SYK—FITC, clone 4D10, anti-Src—PE, clone MOL 171, anti-BTK-Alexa647, clone 53/BTK, anti-PLCγ2-Alexa647, clone K86-1161, anti-BLNK-Alexa488, clone 2B11, anti-AKT-PE, clone 55/PKBa/Akt (all from BD Biosciences). For total ERK and NF-KB detection we used primary purified anti-ERK1/2 (polyclonal) and anti- NF-KB, clone D14E12, both from Cell Signaling Technology and subsequent staining with a secondary goat anti-rabbit antibody Pacific-Blue conjugate (ThermoFisher Scientific). A summary of the stimulation protocol and phosflow staining panel is schematically summarized in Supplementary Figure 1. In all experiments, samples were acquired within 2 h after staining, in a BD LSR II flow cytometer.

Statistical analysis of phosphoflow cytometry data

Signaling analysis was performed in Cytobank (Mountain View, CA, USA) and FlowJo 9.7.6 softwares (Ashland, OR, USA). In brief, *ex vivo*-induced phosphorylation was defined as the fold change of phosphoprotein median fluorescence intensity in stimulated cells compared with unstimulated cells utilizing the hyperbolic sine (arcsinh) scale, which allows the comparison of negative values, often generated in BD LSR II machines after spectral compensation, and corrects large variations in fluorochromes.[27] Basal phosphorylation was quantified as the arcsinh fold difference of malignant and HD B-cells from a healthy-donor sample, which was excluded from further statistical analyses. Through this normalization method we were able to limit variations occurring between different flow cytometry acquisitions and also sustain the same quantification scale in both basal and induced signaling. Detailed description of statistical analysis is described in all figure legends. Unsupervised clustering analysis of phosphosignatures was performed by Ward's method and implemented in the R statistical computing environment. More specifically, the dissimilarity between patient and HD pairs was measured by the euclidean distance of the average phospho-protein response measurements using R's 'dist' function. The dissimilarity matrix was clustered according to Ward's variance minimization (ward.D) using R's 'hclust' function. We then transformed the 'hclust' output using the 'as.dendrogram' function and reordered according to the average phsopho-protein response. The data and analysis are displayed as a heat map and dendrogram using R's 'heatmap.2'.

Cell survival analysis

WM mononuclear cells derived from samples with >70% tumor involvement were seeded in 96-well plates in a density of 10^5 cells/well and treated with 0.05—10 μM dasatinib, tamatinib, ibrutinib or dimethyl sulfoxide for 24 h at 37 °C. Apoptosis was assessed using Annexin-V (BD Biosciences) and 4,6-diamidino-2-phenylindole co-staining to detect early and late apoptotic cells.

Immunohistochemistry

Formalin-fixed, paraffin-embedded bone marrow sections from nine WM patients were recruited from the pathology archives and stained for pSYK (Tyr525/526) and clone C87C1 (Cell Signaling Technology). Staining was performed with the Bond Max Autostainer (Leica Biosystems, Buffalo Grove, IL, USA). Tyramide signal amplification (TSA) technology was applied to unmask dim SYK phosphorylation. Pictures were taken on an Axioplan 2 microscope (Zeiss Microscopy, Jena, Germany).

Real-time polymerase chain reaction

IgM+ cells were isolated from WM and HD samples through magnetic cell sorting with anti-human IgM microbeads (Miltenyi Biotec, Auburn, CA, USA) and stored in Trizol at − 80 °C. RNA was extracted as per the manufacturer's protocol. complementary DNA was synthesized with the SuperScript VILO kit (Invitrogen Biosource). μ-chain messenger RNA (mRNA) was quantified using the following primer set: 5′-CGTGTCCGAAGAGGAATGG- 3′, 5′-AGAGGCTCAGGAGGAAGAGG-3′, which specifically amplifies surface μ-chain transcripts. Real-time quantitative PCR was performed on QuantStudio 7 flex System (ThermoFisher Scientific) with SYBR Green (Life Technologies) and TaqMan Universal PCR Master Mix (Applied Biosystems). GAPDH was used as a housekeeping control gene (human GAPDH endogenous control, ThermoFisher Scientific). The reaction was performed in duplicate and relative amounts of mRNA transcripts were corrected for the purity of the sample for IgM+ cells and calculated by the comparative ΔCt method using the formula: relative expression = $2^{\Delta Ct}$/ α, where α is the sample's IgM+ cell purity after magnetic sorting. sIgM was measured before magnetic sorting by flow cytometry to correlate mRNA to protein levels.

MYD88-CD79A/B sequencing and IGHV mutation status

Genomic DNA obtained from WM mononuclear cells was sequenced for the entire coding region of MYD88, CD79A and CD79B in the context of deep targeted sequencing of 374 genes recurrently mutated in cancer (FoundationOne Heme). The presence of MYD88 L265P was also verified with an allele-specific polymerase chain reaction, as previously described.[29] IGHV mutation analysis was performed using a combination of PCR/fragment analysis to detect the clonal IGHV rearrangement followed by sequence analysis to determine the IGHV mutation frequency (Cancer Genetics, Inc).

Statistical analysis

Statistical analyses were performed using Prism 6.0 software (La Jolla, CA, USA). We applied two-tailed Mann–Whitney test and ordinary analysis of variance test for non-paired multiple comparisons, whereas for paired samples we applied Wilcoxon test and repeated-measures analysis of variance with Tukey's multiple comparison. Correlations were assessed with Pearson or Spearman tests. Association with stable or progressive disease was assessed with X^2 test and time to second line treatment differences were assessed with log-rank test. Sample size for basal and anti-IgM induced phosphorylation studies was based on previous phosphoflow studies on aberrant BCR signaling.[27] Statistical significance was defined as $P < 0.05$. Figures represent means ± s.e.m. values. All statistical tests are mentioned in detail in Figure legends.

RESULTS

WM cells exhibit constitutive activation of BCR-related signaling elements

We first examined primary WM cells in the absence of exogenous stimuli and assessed basal phosphorylation levels for the following signaling molecules: SFK, SYK, BTK, BLNK, PLCγ2, ERK, NF-κB and AKT. WM cells exhibited at variable degrees, significantly higher levels of constitutive phosphorylation for all eight signaling proteins compared with normal peripheral blood B-cells (Figure 1a). Higher levels of basal phosphorylation were also observed compared with HD bone marrow CD20+CD10- mature B-cells and CD138+ plasma cells (Supplementary Figure 2A). Total protein levels did not differ between WM and normal B-cells, yet showed higher expression variability. BTK in particular showed a lower expression trend in WM cells, which nevertheless did not reach statistical significance (Supplementary Figure 2B). We next sought to validate the presence of constitutive *in vivo* BCR activation in fixed tissues. Immunohistochemical staining confirmed the presence of high levels of phosphorylated SYK in clonal infiltrates found in WM bone marrow biopsy sections (Figure 1b). Utilizing pPLCγ2 as the main read-out, due to its central localization within the pathway, we observed that basal phosphorylation in WM cells was attenuated on 60 min of proximal kinase preinhibition, utilizing inhibitors for SFK (dasatinib), SYK (tamatinib) and BTK (ibrutinib; Figure 1c, Supplementary Figure 3A). In addition, we evaluated the *in vivo* effects of Ibrutinib treatment on basal BCR signaling in matched samples obtained before ibrutinib and after 6 months of daily ibrutinib therapy, from eight patients enrolled in the clinical trial NCT01614821 and observed a decline in constitutive pPLCγ2

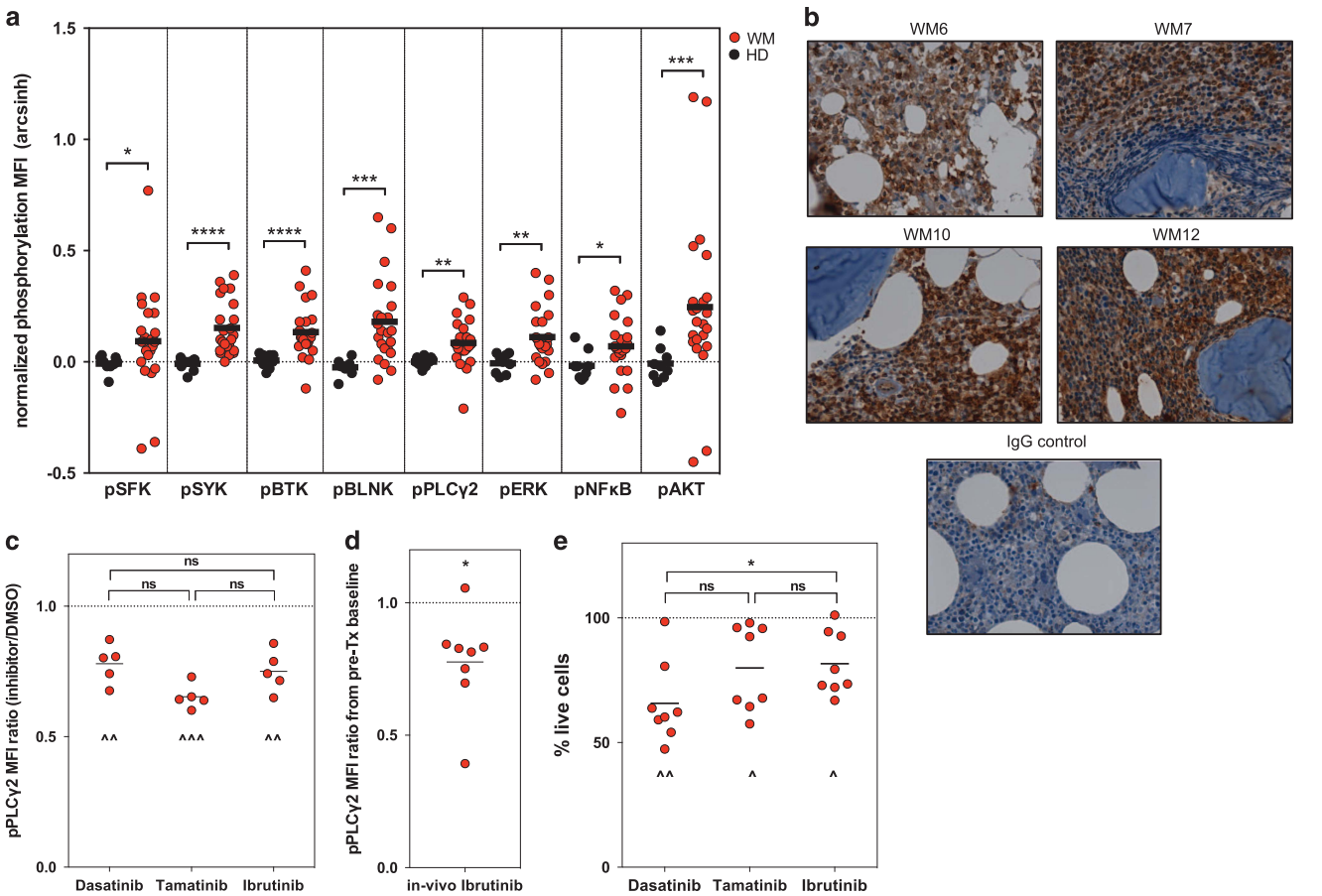

Figure 1. WM cells exhibit constitutive activation of the BCR pathway. (**a**) Differences in basal levels of phosphorylation between HD B cells (black) and WM cells (red) expressed in arcsinh scale (HD $n = 9$, WM $n = 23$, $^{****}P < 0.0001$, $^{***}P < 0.001$, $^{**}P < 0.01$, $^{*}P < 0.05$, Mann–Whitney test). (**b**) representative WM bone marrow sections stained for pSYK (Immunohistochemistry-tyramide signal amplification technology, ×40). (**c**) Inihbition of basal levels of pPLCγ2, assessed 60 min after *in vitro* preinhibition with Dasatinib (10 μM), Tamatinib (10 μM) and Ibrutinib (10 μM), illustrated as a ratio from dimethyl sulfoxide (DMSO) treated matched control samples (WM $n = 5$, Repeated measures analysis of variance (ANOVA) with Tukey's multiple comparison test, $^{\wedge\wedge}P < 0.01$, $^{\wedge\wedge\wedge}P < 0.001$, ^ represents significant difference from DMSO matched control). (**d**) Inhibition of basal levels of pPLCγ2 at 6 months of continuous ibrutinb treatment in eight WM patients, as a ratio from pre-ibrutinib phosphorylation levels (WM $n = 8$, Wilcoxon test, $^{*}P < 0.05$, * represents significant difference from pre-ibrutinib treatment matched samples). (**e**) Viability of WM mononuclear cells assessed after 24 h of treatment with Dasatinib (1 μM), Tamatinib (1 μM) and Ibrutinib (1 μM). Viability is normalized to DMSO treated control. (WM $n = 8$, Repeated measures ANOVA with Tukey's multiple comparison test, $^{\wedge}P < 0.05$, $^{\wedge\wedge}P < 0.01$, ^ represents significant difference from DMSO matched controls, $^{*}P < 0.05$, * represents significant difference in matched samples among different inhibitors).

(Figure 1d, Supplementary Figure 3b). One patient (WM7) showed no attenuation in BCR signaling and this patient was the only one with a significant expansion of clonal cells on treatment, despite a drop in serum IgM and amelioration of clinical symptomatology. Although *in vitro* and *in vivo* inhibition appear as minimal numerically, basal phosphorylation values in primary unfixed cells are expectedly low and as a result phosphorylation inhibition appears as 'incomplete', given the remaining background. To prove the functional significance of constitutive signaling in WM cells we evaluated the consequences of 24 h proximal kinase inhibition in primary WM samples and observed significantly decreased viability, with dasatinib showing the highest efficacy (Figure 1e, Supplementary Figure 3C).

BCR crosslinking elicits augmented phosphoresponses in WM cells

The presence of basal BCR signaling activation, which was essential for WM cell survival, served as first evidence of potentiated signaling *in vivo*. However, since all the signaling proteins that were interrogated constitute members of other signaling pathways, including TLR/MYD88 and CXCR4, we sought to directly examine the capacity of WM cells to signal through the BCR pathway, utilizing well established *ex vivo* BCR stimulation assays. Normal and malignant B cells were therefore stimulated by sIgM crosslinking with 10 μg/ml soluble polyclonal anti-μ specific $F(ab')_2$ fragments for 4 min. As previously documented, sIgM crosslinking in normal B-cells elicits minimal to moderate phosphoresponses, in the absence of concomitant phosphatase inhibition.[6,28] In contrast, sIgM crosslinking of WM cells showed significantly augmented BCR signaling capacity through SFK, SYK, BLNK, PLCγ2 and ERK (Figure 2a). WM cells exhibited similarly hightened phosphoresponses compared with mature B-cells and plasma cells (Supplementary Figure 4). Interestingly, except in a few patients, BTK, NF-κB and AKT were not highly activatable from their already high basal state, despite being parts of canonical BCR signaling. As PLCγ2 had the highest phosphorylation fold change, we tested if TLR stimulation had similar effects on PLCγ2 activation considering that both the BCR and TLR pathway share proximal signaling nodes. Nevertheless, TLR stimulation failed to activate PLCγ2 and did not exhibit any synergy on concomittant BCR stimulation (Supplementary Figure 5).

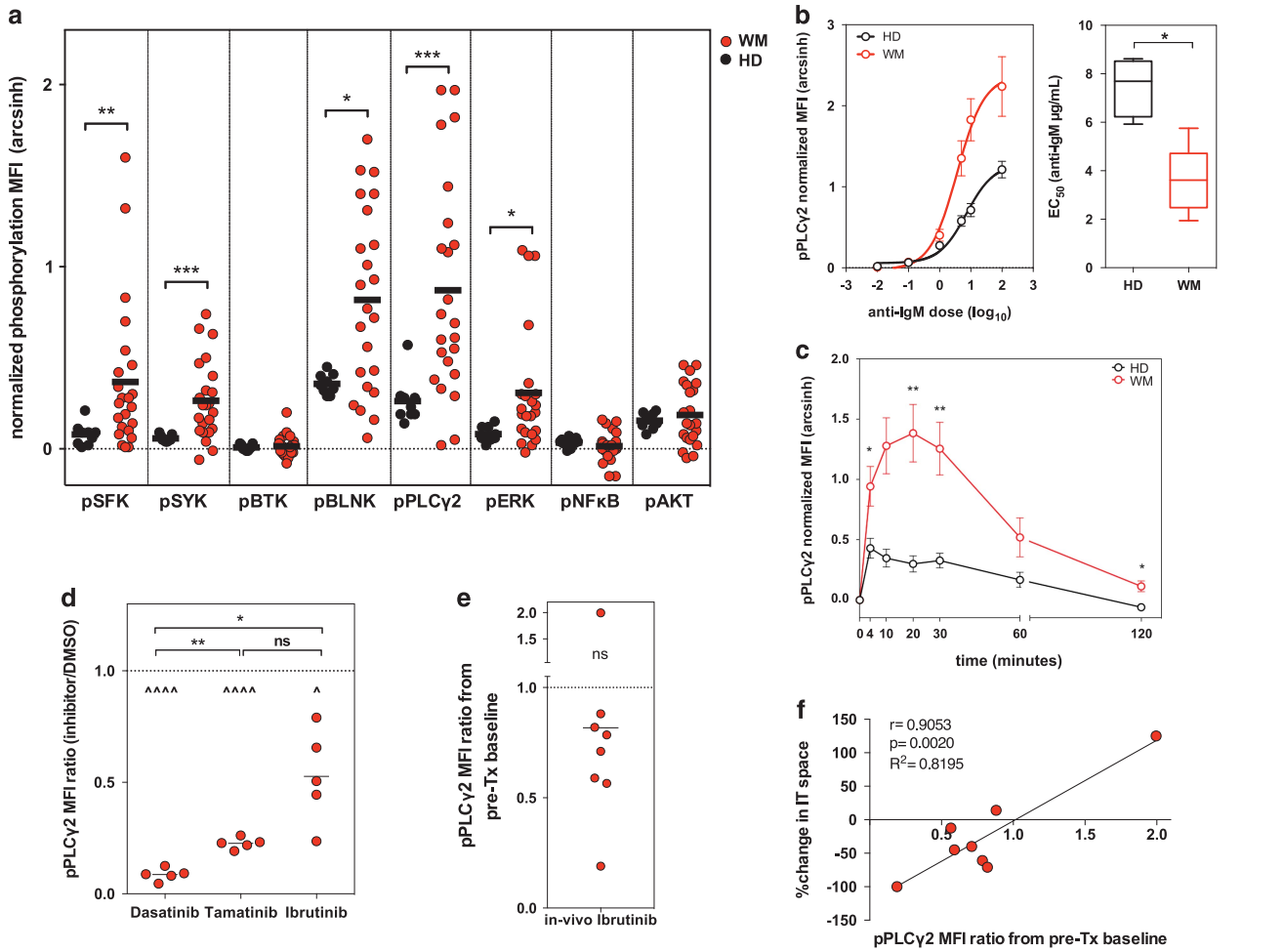

Figure 2. BCR crosslinking elicits augmented phosphoresponses in WM cells. (**a**) anti-IgM induced fold change in phosphorylation in HD B-cells (black) and WM cells (red) expressed in the arcsinh scale (HD $n=9$, WM $n=23$, $^{***}P<0.001$, $^{**}P<0.01$, $^{*}P<0.05$, Mann–Whitney test). (**b**) Dose response of anti-IgM induced fold change in pPLCγ2 in HD (black) and WM (red) cells and EC_{50} values of all individuals (HD $n=4$, WM $n=5$, $^{*}P<0.05$, Mann–Whitney test). (**c**) Kinetics of anti-IgM induced fold change in pPLCγ2 in HD (black) and WM (red) cells. At 0, fold change is 0 by definition. (HD $n=4$, WM $n=6$, $^{**}P<0.01$, $^{*}P<0.05$, Mann–Whitney test). (**d**) Inhibition of anti-IgM induced pPLCγ2. Stimulation was performed for 4 min after a 60 min *in vitro* preinhibition with Dasatinib (10 μM), Tamatinib (10 μM) and Ibrutinib (10 μM). Here illustrated as a ratio from dimethyl sulfoxide (DMSO) treated matched control samples (WM $n=5$, repeated measures analysis of variance (ANOVA) with Tukey's multiple comparison test, $^{\wedge}P<0.05$, $^{\wedge\wedge\wedge\wedge}P<0.0001$, ^ represents significant difference from DMSO matched control, $^{*}P<0.05$, $^{**}P<0.01$, * represents significant difference in matched samples among different inhibitors). (**e**) Inhibition of anti-IgM induced pPLCγ2 at 6 months of continuous ibrutinb treatment, as a ratio from pre-ibrutinib matched anti-IgM induced pPLCγ2 levels (WM $n=8$, Wilcoxon test). (**f**) correlation between anti-IgM induced pPLCγ2 ratio and percentage change in intratrabecular (IT) space clonal infiltration post-ibrutinib treatment (Pearson test).

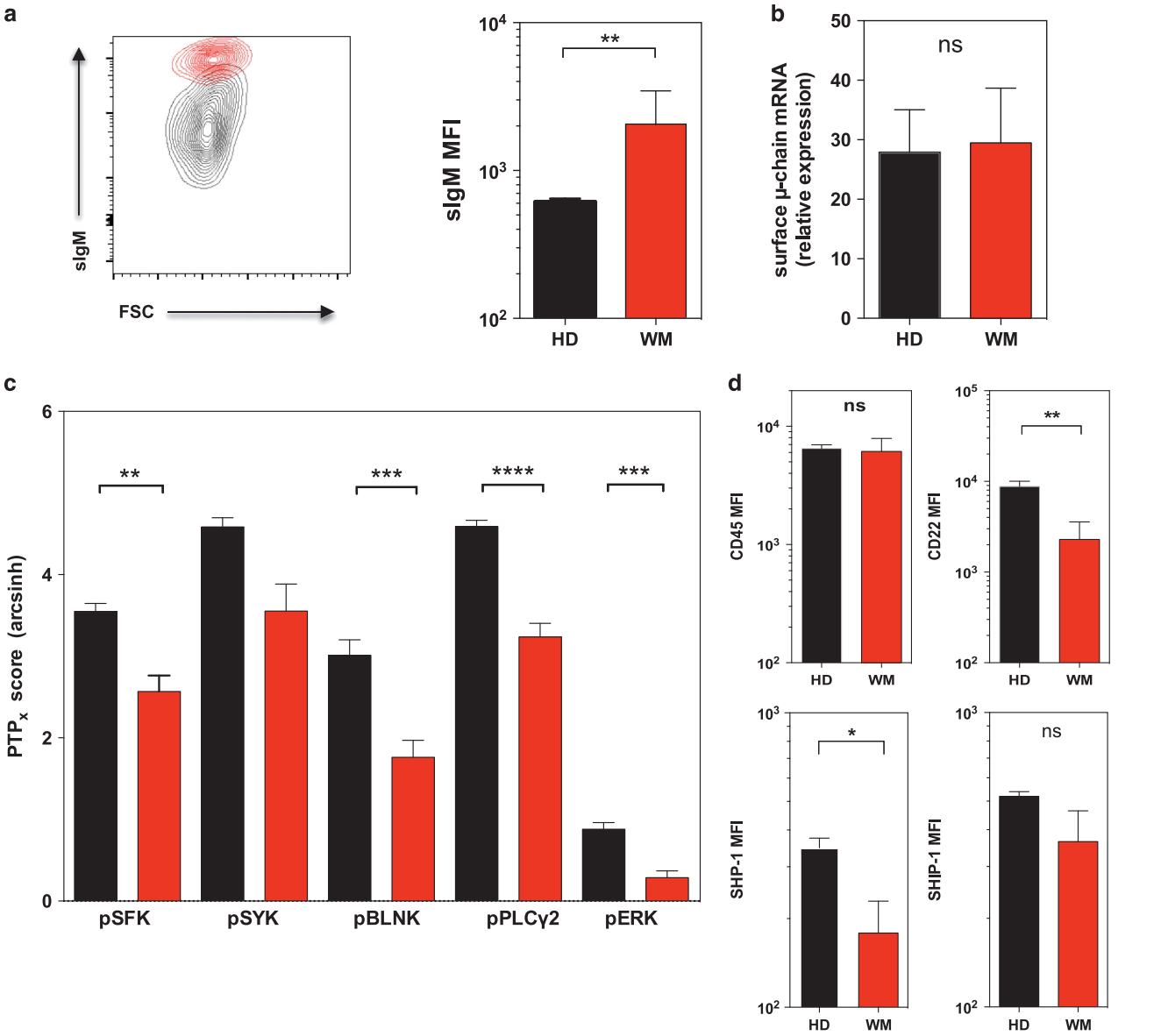

Figure 3. WM cells express higher levels of the receptor and show loss of phosphatase activity compared with HD cells. (**a**) sIgM overlayed cluster plots (left) for HD IgM+ B-cells (black) and WM (red) cells and bar graphs for all tested individuals (HD $n=4$, WM $n=11$, $^{**}P<0.01$, Mann–Whitney test). (**b**) Surface μ-chain mRNA level relative expression in IgM+ HD ($n=4$) B-cells and WM ($n=8$) cells. Human GAPDH was used as an endogenous control (Mann–Whitney test). (**c**) Phosphatase score for HD B-cells (black) and WM cells (red) $PTP_X = pX\ (\text{arcsinh fold change})_{\text{algM+H2O2}}$—$pX(\text{arcsinh fold change})_{\text{algM}}$, where pX is any phosphoprotein (HD $n=9$, WM $n=23$, $^{****}P<0.0001$, $^{***}P<0.001$, $^{**}P<0.01$, Mann–Whitney test). (**d**) Surface CD45 median fluorescence intensity (MFI) and surface CD22 MFI in HD ($n=4$) B-cells and WM ($n=11$) cells. Intracellular SHP-1 and intracellular SHIP-1 MFI in HD ($n=4$) B-cells and WM ($n=6$) cells. MFI is normalized to an FMO (fluorescence minus one) control.

Besides the high-signaling amplitude observed with a high dose of anti-IgM, dose-response experiments, showed that WM cells, exhibited lower EC_{50} values than HD B-cells ($EC_{50\text{-HD}}$: 7.23 ± 1.22 μg/ml, $EC_{50\text{-WM}}$: 3.63 ± 2.39 μg/ml; Figure 2b), suggesting the presence of a receptor which is more sensitive to exogenous stimuli. Moreover, the high deviation in sensitivity among WM samples could be an effect of differential expression of sIgM. Furthermore, beyond the time point of 4 min, WM PLCγ2 showed distinct phosphorylation kinetics characterized by prolonged hyperactivation, reaching a maximum within 20 min post-stimulation, while significant levels of phosphorylation were detectable even 120 min post-stimulation (Figure 2c). SYK and BLNK displayed similar phosphorylation kinetics to PLCγ2. BTK, AKT and NF-κB showed minimal fold changes in phosphorylation from baseline during the course of 120 min, yet BTK signal was maintained longer in WM cells compared with normal B cells (Supplementary Figure 6). Overall, this ongoing signaling propagation is suggestive of active positive feedback mechanisms or defective negative feedback at the level of proximal kinases. *In vitro* inhibition before anti-IgM stimulation attenuated the signaling potential of WM cells. Treatment with dasatinib, tamatinib and ibrutinib showed an escalating potency, with dasatinib resulting in complete signal inhibition while ibrutinib showed only partial inhibition of PLCγ2 activation. (Figure 2d, Supplementary Figure 7A). In WM cases with significant tumor burden we evaluated the inhibitory potential to anti-IgM stimulation of all three inhibitors in doses spanning from 0.1 to 100 μM, and observed that SFK blockade is the most potent one even at the lowest inhibitor concentration (Supplementary Figure 7B). Thus, optimal inhibition in the presence of a cross-linked receptor can only be performed at the most proximal

kinase level. In agreement with these findings, anti-IgM stimulated WM cells of patients on active ibrutinib therapy showed a moderate, yet not complete, inhibition in their phosphoresponses compared with their pre-treatment phospho-response baseline (Figure 2e, Supplementary Figure 7C). Patient WM7 who failed to show a decrease in basal pPLCγ2 and exhibited a clonal expansion while on ibrutinib, exhibited an enhanced phospho-response on anti-IgM stimulation. Moreover, malignant cell phosphoresponses showed a strong correlation with changes observed in bone marrow tumor involvement for those patients on ibrutinib, thereby providing a link between the attenuation of BCR signaling potential and the *in vivo* tumoricidal effects elicited by BTK inhibition (Figure 2f). The CXCR4 status of these patients showed no correlation with the inhibitory capacity of *in vivo* ibrutinib on their BCR phosphoresponses.

WM cells express high levels of sIgM and show loss of phosphatase activity

Given that WM cells have strong BCR phosphosignatures, in the absence of recurrent BCR signaling mutations, we next examined the expression levels of the BCR in WM cells. We observed that WM cells expressed significantly higher levels of sIgM with a prominent narrow distribution versus IgM+ normal B-cells, which as expected constituted the majority of circulating HD B-cells (Figure 3a). Of note the sizes of WM and HD B-cells were relatively similar (according to forward scatter measurements as reported in Figure 3a), showing that the surface density of sIgM was higher in WM versus HD B-cells. WM cells also expressed higher sIgM compared with mature marrow B-cells and plasma cells (Supplementary Figure 8A). In addition to the protein levels of sIgM, we quantified the levels of the membrane specific transcript of μ chain. Interestingly we observed no difference in μ-chain mRNA between HD B-cells and WM cells; and no protein–mRNA correlation among WM samples (Figure 3b, Supplementary Figure 8B), suggesting that posttranslational modifications result in high sIgM expression in WM cells.

Besides the increased receptor density, an alternative mechanism of hyperstimulation could be the loss of regulation by phosphatases. We therefore developed a method for the quantification of phosphatase input on signaling, by assessing the net benefit in signaling magnitude after the chemical inactivation of all phosphatases. sIgM crosslinking in the presence of low doses of H_2O_2, a potent pan-phosphatase inhibitor, is proven to dramatically enhance the capacity of B-cells to signal through the BCR pathway.[6] As shown in a representative sample in Supplementary Figure 8C HD B-cells tend to show minimal responses on BCR stimulation while BCR stimulation with concomitant phosphatase inhibition drastically increases their responsiveness. This suggests that physiological BCR signaling is under robust phosphatase regulation. WM cells on the other hand are more responsive to BCR stimulation alone and although concomitant phosphatase inhibition renders them more responsive, the net benefit from this inhibition is lower compared with HD B-cells, given that the signal is not maximized at a dose of 3.3 μM of H_2O_2 (maximization occurs at H_2O_2 doses >33 μM, Supplementary Figure 8D). Interestingly WM cells lag in terms of responsiveness even at very high doses of H_2O_2. Therefore, considering that the net BCR signaling benefit occurring with the addition of H_2O_2 provided an indirect measurement of phosphatase activity, we scored the net effect of phosphatases on hyper-stimulatable proteins as the difference $PTP_X = pX(\text{arcsinh fold change})_{\text{aIgM+H2O2}} - pX(\text{arcsinh fold change})_{\text{aIgM}}$, where pX is any phosphoprotein. These studies revealed a significant loss of phosphatase regulation on SFK, BLNK, PLCγ2 and ERK, offering an additional explanation for augmented BCR signaling in WM (Figure 3c). It is known that BCR signaling is regulated by CD45, a transmembrane protein with cytoplasmic tyrosine phosphatase activity, and CD22, a transmembrane lectin interacting with intracellular phosphatases, primarily SHP-1 and SHIP-1. In support of our signaling findings, WM cells showed a downregulation of CD22 and SHP-1 expression while no difference was observed in CD45 and SHIP-1 expression (Figure 3e).

Intra-WM signaling heterogeneity correlates with distinct clinical outcomes and differential BCR expression

As shown in Figure 2a, considerable variability in BCR signaling was observed in WM patients versus normal B-cells. We therefore quantified this variability by computing the variance of the median phosphoresponses across our set of patients and healthy individuals (Figure 4a). We found that the elevated diversity among WM patients was centered on canonical BCR signaling elements: pSFK, pSYK, pBLNK, pPLCγ2, pERK and pAKT. Furthermore, we tested whether intrapatient heterogeneity preserved the structure of the BCR signaling pathway. Explicitly, we conjectured that patients with higher median pSFK would also have higher levels of pSYK, pPLCγ2 and so on. We tested this hypothesis by analyzing the spearman correlation between median phosho-responses among WM patients and HDs. Qualitatively, Figure 4b shows that the set of WM phosphoresponse correlations did not align with those from the HD set. Notably the correlation between pBLNK and pERK, pSFK, pSYK or pPLCg2 was from negative or null among HDs and positive among patients. This difference in the correlations suggests that distinct BCR signaling properties are present in WM patients versus HDs.

We next investigated whether the diversity in WM patients contained patient groups with unique signaling properties. We tested this hypothesis by using agglomerative clustering (Ward's method) of the median arcsinh phosphorylation of proteins with the highest intra-WM variance on anti-IgM stimulation (Figure 4c). Ward's method of agglomerative clustering extended our intuition by merging groups of patients whose variance in their median phosphoresponse to anti-IgM is minimized (Figures 4a and b). Through this clustering analysis we identified three unique clusters denoted as A, B and C. Clusters A and B were comprised of a group of patients with high phosphoprofiles (high-profile group), whereas cluster C showed phosphoprofiles indistinguishable from healthy individuals (healthy-like-profile group; Figure 4c). Importantly those patients with high phosphoprofiles were characterized as experiencing ongoing disease progression at the time of WM cell collection while those with healthy-like phosphoprofiles were more likely to be in a stable disease state (Figure 4d). In addition, the healthy-like group of patients exhibited delayed time to second line treatment, as assessed retrospectively from diagnosis to the date of sample collection (Figure 4e). When analyzed separately, clusters A and B of the high phosphoprofile group had no differences in terms of clinical outcome. Between the two WM groups, sIgM expression was found to be significantly higher in the 'high' phosphoprofile group while no difference was observed in phosphatase activity (Figure 4f and g). Moreover, no difference was observed between the two signaling groups in regards to their MYD88 mutation status as all patients screened were MYD88 L265P positive, or their CD79A/B mutation status, with only one patient in the high group carrying a CD79B Y196C mutation. Of note, this patient was characterized by aggressive clinical course and WM cells were derived from a lymphomatous pleural effusion. Finally, no difference was observed between the two groups in terms of their IGHV mutation status (Supplementary Figure 9).

DISCUSSION

WM is a lymphoid neoplasm with low occurrence of BCR-signaling-associated mutations. We report here our finding of high basal phosphorylation of multiple BCR-related proteins using phospho-flow cytometry and immunohistochemistry thereby providing

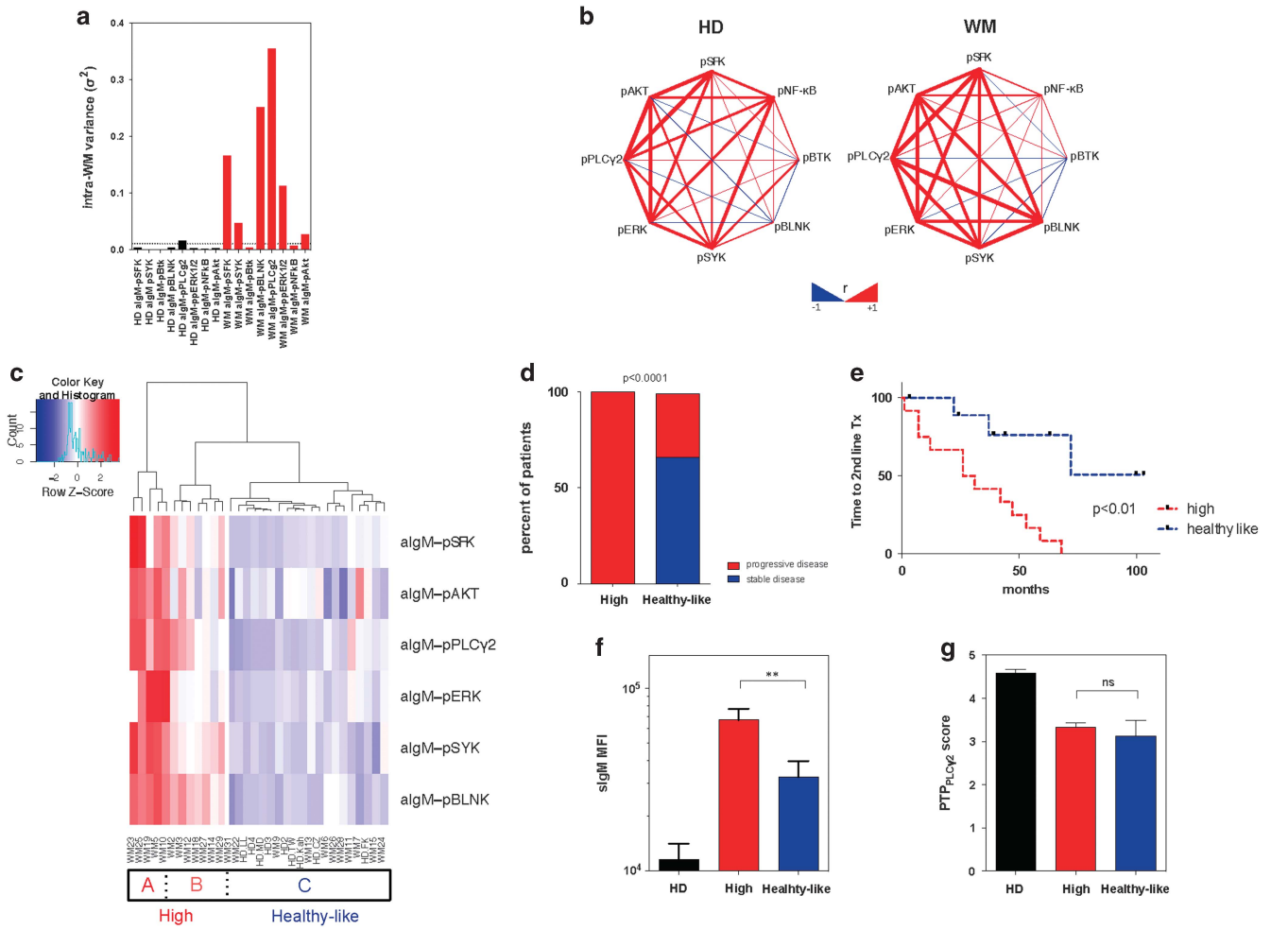

Figure 4. Intra-WM signaling heterogeneity is driven by differential BCR expression and correlates with distinct clinical outcomes. (**a**) Intra-WM anti-IgM-induced phophoprotein variance (HD, black; WM, red). (**b**) Inter-phosphoprotein Spearman correlation network analysis (positive correlations, red; negative correlations, blue). (**c**) Agglomerative clustering analysis for 23 patients interrogated for all six phosphoproteins on IgM crosslinking. (**d**) Patient status on sample collection (χ^2 test $P < 0.0001$). (**e**) Time to second line treatment from diagnosis date to sample collection date (log-rank survival analysis). (**f**) sIgM levels among groups (HD $n = 4$, WM_{high} $n = 6$, $WM_{healthy\text{-}like}$ $n = 5$, $^{**}P < 0.01$, analysis of variance (ANOVA) test). (**g**) Phosphatase score for pPLCγ2 among groups (HD $n = 9$, WM_{high} $n = 13$, $WM_{healthy\text{-}like}$ $n = 10$, ANOVA test).

evidence of *in vivo* BCR stimulation in WM. Constitutive BCR signaling appears to be sensitive to *in vitro* and *in vivo* proximal kinase inhibition, in support of the application of BCR inhibitors for the treatment of WM. In previous studies, constitutive activation of distal signaling proteins, including NF-κB, ERK and AKT, have been attributed to the MYD88 L265P and CXCR4-WHIM-like mutations, while at the proximal level, BTK activation has been shown to interact with the mutated MYDosome of WM cells.[15,23,30] The latter supported the therapeutic rationale of targeting BTK with ibrutinib in WM patients. Recently, fostamatinib, the precursor molecule of tamatinib, was shown to have *in vitro* tumoricidal activity against WM cells.[22] However, none of the above-mentioned proteins are solely driven by the BCR. For instance, TLR/MYD88 activation in human B-cells, besides its canonical axis, has been shown to activate through the adapter DOCK8, an alternative SFK-SYK route, which further enhances B-cell activation.[31]

To comprehend the net contribution of the BCR in basal protein activation, we interrogated the *ex vivo* capacity of clonal cells to respond to anti-IgM stimulation. Under that prism WM cells appeared hyperresponsive through SFK, SYK, BLNK, PLCγ2 and ERK compared with normal B-cells, while BTK was the only signalosome component that did not follow this hyperactivated cascade. Furthermore, the hyperactivation of distal molecules like PLCγ2 and ERK, independently of BTK, suggests a redundant role of BTK in the propagation of BCR-driven signals. In favor of that scenario, the *in vitro* preinhibition of BTK with ibrutinib showed only partial inhibition of PLCγ2 activation on anti-IgM stimulation, as opposed to the strong inhibition imposed by dasatinib and tamatinib. Furthermore, although ibrutinib is an irreversible inhibitor of BTK, samples from patients actively treated with ibrutinib, showed only a partial abrogation of *ex vivo* activated PLCγ2. Indeed, although BTK directly activates PLCγ2, it is known that SYK can also indirectly activate PLCγ2, by phosphorylating BLNK.[32–34] Our findings may explain why, while WM patients show very good clinical responses to ibrutinib, they did not achieve complete responses, maintaining significant amounts of clonal cells in their marrows post-treatment (Table 2, Figure 2f).[24] A clinical consequence of our findings would be to examine SFK and SYK as additional targets for the treatment of WM, especially in conjunction with inhibitors of the TLR axis. Moreover, the full elucidation of cross-talk between BCR and TLR signaling is still a subject to be explored. In our study LPS stimulation failed to generate detectable PLCγ2 phosphorylation, therefore it would be interesting to study the BCR-driven activation of molecules such as TRAF6 and TAK1 which are shown to be activated by MYD88 L265P.[35]

Ex vivo sIgM crosslinking, in the absence of phosphatase inhibition by H_2O_2, generated minimal phosphoresponses in healthy B cells.[6] The fact that WM cells respond with high

amplitude, sensitivity and in a prolonged fashion suggested the presence of increased input by positive and/or decreased input by negative signaling regulators. In accordance with this potentiated signaling phenotype, we found that WM cells express higher levels of sIgM compared with IgM+ normal B-cells. Aberrant receptor expression has been previously described in multiple lymphoid neoplasms as a mechanism of signaling enhancement, particularly for multiple cytokine receptor pathways.[36,37] Increased BCR expression has been previously described in activated B-cell-like diffuse large B-cell lymphoma cell lines as a consequence of CD79A and CD79B immunoreceptor tyrosine-based activation mutations, which result in decreased internalization of sIgM.[10] Although it is not clear if high sIgM in WM is an epiphenomenon of increased expression or loss of internalization, considering the relatively low frequency of BCR-related mutations in WM, these findings demonstrate that increased pathway activity can arise in the absence of signaling-associated genetic alterations. The absence of correlating high-surface μ-chain mRNA suggests the existence of posttranslational modifications leading to aberrant protein expression, such as N-glycosylation, which has been reported in CLL and follicular lymphoma.[38,39] Simultaneously, WM cells exhibit significant loss of phosphatase activity, as shown by decreased signaling maximization, when stimulated through the BCR in the presence of H_2O_2, a phenomenon which could be partially attributed to the decreased expression of inhibitory molecules CD22 and SHP-1. This is compatible with the current models of lymphomagenesis, since phosphatase loss has been documented to occur in multiple lymphoid neoplasms secondary to genetic or epigenetic alterations, leading to dysregulated intracellular signaling.[40,41] Moreover, it is noteworthy that increased BCR responsiveness, with minimal H_2O_2 signaling enhancement compared with normal germinal center IgM+ cells, and concomittant downregulation of CD22 and SHP-1, with normal SHIP-1 expression, have been recently shown in IgM+ follicular lymphoma cells.[42] Although the sequence of the above-mentioned events is not clear yet, sIgM upregulation and phosphatase loss could both shape the hyperactive BCR network we described.

Like all indolent B-cell non-Hodgkin's lymphoma, WM is characterized by high heterogeneity in terms of clinical presentation.[43] However, limited biological parameters have been associated so far with the aggressiveness of the disease, mostly due to the fact that pre-clinical studies have been based on WM cell lines and not primary samples from larger patient pools. To approach intra-WM heterogeneity we generated BCR phosphosignatures comprised of the highly variable phosphoresponses that patients demonstrated for pSFK, pSYK, pBLNK, pPLCγ2, pERK and pAKT. Agglomerative clustering analysis partitioned our cohort into a 'high' and a 'healthy-like' signaling profile, with the latter being linked to a significantly more indolent clinical phenotype. This could suggest that BCR signaling is highly utilized in more aggressive disease subtypes, while it remains well controlled in slowly progressing subtypes. Interestingly, higher sIgM expression correlated with the 'high' signaling group, while phosphatase activity was similarly low between the two groups, showing that phosphatase loss is not sufficient to fully potentiate signaling, and that the main driver of BCR hyperactivation is the receptor. Moreover, the fact that the 'healthy-like' group presents a similar signaling capacity with healthy B cells, despite higher BCR expression and lower phosphatase activity, suggests that WM cells in indolent subtypes, may have anergic features, a phenomenon previously described in the mutated-subtype of CLL, which is less aggressive, compared with the unmutated-subtype, which is fully responsive on BCR stimulation.[44]

Our findings demonstrate the occurrence of chronic active signaling in WM. From a mechanistic perspective, it is still unclear if high BCR utilization is antigen-dependent or independent. No evidence exists to-date regarding potential antigen candidates in WM, contrary to CLL and marginal zone lymphoma subtypes.[45–47] One could envision that structural features of the BCR, like N-glycosylation or specific CDR3 amino acid sequences, as in follicular lymphoma and CLL, could favor BCR aggregation and autonomous signaling.[13,38,39] Finally, from a therapeutic perspective, it is clear that there is a need for optimization in BCR-directed therapies in WM, especially in patients with a more aggressive disease, who seem highly dependent on BCR signaling.

CONFLICT OF INTEREST

The authors declare no conflict of interest.

ACKNOWLEDGEMENTS

We would like to thank Dr Katya Manova, Dmitry Yarilin and Mesruh Turkekul from the Molecular Cytology Core Facility at Memorial Sloan Kettering Cancer Center for the help with immunohistochemistry studies. This work was supported by The Lymphoma Foundation and NIH U54 CA148967 fund. KVA is supported by a SASS Medical Foundation Post-Doctoral Research Fellowship.

AUTHOR CONTRIBUTIONS

KVA, RV, GAB, ZRH, SPT, MRMvdB and MLP were responsible for the conception and design of the study. KVA, EV and MC performed the experiments. AD, MP, CM and KK were involved in the acquisition of patient material. KVA, RV, CZ, GAB, AD, MRMvdB and MLP were involved in the analysis and interpretation of data, RV and CZ were involved in the computational analysis of data, KVA, RV, GAB, ZRH, SPT, MRMvdB and MLP wrote the manuscript.

REFERENCES

1 Kraus M, Alimzhanov MB, Rajewsky N, Rajewsky K. Survival of resting mature B lymphocytes depends on BCR signaling via the Igalpha/beta heterodimer. *Cell* 2004; **117**: 787–800.
2 Rajewsky K. Clonal selection and learning in the antibody system. *Nature* 1996; **381**: 751–758.
3 Fu C, Turck CW, Kurosaki T, Chan AC. BLNK: a central linker protein in B cell activation. *Immunity* 1998; **9**: 93–103.
4 Baba Y, Hashimoto S, Matsushita M, Watanabe D, Kishimoto T, Kurosaki T *et al.* BLNK mediates Syk-dependent Btk activation. *Proc Natl Acad Sci USA* 2001; **98**: 2582–2586.
5 Beitz LO, Fruman DA, Kurosaki T, Cantley LC, Scharenberg AM. SYK is upstream of phosphoinositide 3-kinase in B cell receptor signaling. *J Biol Chem* 1999; **274**: 32662–32666.
6 Irish JM, Czerwinski DK, Nolan GP, Levy R. Kinetics of B cell receptor signaling in human B cell subsets mapped by phosphospecific flow cytometry. *J Immunol* 2006; **177**: 1581–1589.
7 Egawa T, Albrecht B, Favier B, Sunshine MJ, Mirchandani K, O'Brien W *et al.* Requirement for CARMA1 in antigen receptor-induced NF-kappa B activation and lymphocyte proliferation. *Curr Biol* 2003; **13**: 1252–1258.
8 Young RM, Staudt LM. Targeting pathological B cell receptor signalling in lymphoid malignancies. *Nat Rev Drug Discov* 2013; **12**: 229–243.
9 Rickert RC. New insights into pre-BCR and BCR signalling with relevance to B cell malignancies. *Nat Rev Immunol* 2013; **13**: 578–591.
10 Davis RE, Ngo VN, Lenz G, Tolar P, Young RM, Romesser PB *et al.* Chronic active B-cell-receptor signalling in diffuse large B-cell lymphoma. *Nature* 2010; **463**: 88–92.
11 Lenz G, Davis RE, Ngo VN, Lam L, George TC, Wright GW *et al.* Oncogenic CARD11 mutations in human diffuse large B cell lymphoma. *Science* 2008; **319**: 1676–1679.
12 Herishanu Y, Perez-Galan P, Liu D, Biancotto A, Pittaluga S, Vire B *et al.* The lymph node microenvironment promotes B-cell receptor signaling, NF-kappaB activation, and tumor proliferation in chronic lymphocytic leukemia. *Blood* 2011; **117**: 563–574.
13 Duhren-von Minden M, Ubelhart R, Schneider D, Wossning T, Bach MP, Buchner M *et al.* Chronic lymphocytic leukaemia is driven by antigen-independent cell-autonomous signalling. *Nature* 2012; **489**: 309–312.
14 Janz S. Waldenstrom macroglobulinemia: clinical and immunological aspects, natural history, cell of origin, and emerging mouse models. *ISRN Hematol* 2013; **2013**: 815325.
15 Treon SP, Xu L, Yang G, Zhou Y, Liu X, Cao Y *et al.* MYD88 L265P somatic mutation in Waldenstrom's macroglobulinemia. *N Engl J Med* 2012; **367**: 826–833.
16 Hunter ZR, Xu L, Yang G, Zhou Y, Liu X, Cao Y *et al.* The genomic landscape of Waldenstrom macroglobulinemia is characterized by highly recurring MYD88 and

WHIM-like CXCR4 mutations, and small somatic deletions associated with B-cell lymphomagenesis. *Blood* 2014; **123**: 1637–1646.
17 Roccaro AM, Sacco A, Jimenez C, Maiso P, Moschetta M, Mishima Y *et al.* C1013G/CXCR4 acts as a driver mutation of tumor progression and modulator of drug resistance in lymphoplasmacytic lymphoma. *Blood* 2014; **123**: 4120–4131.
18 Poulain S, Roumier C, Galiegue-Zouitina S, Daudignon A, Herbaux C, Aiijou R *et al.* Genome wide SNP array identified multiple mechanisms of genetic changes in Waldenstrom macroglobulinemia. *Am J Hematol* 2013; **88**: 948–954.
19 Ciric B, VanKeulen V, Rodriguez M, Kyle RA, Gertz MA, Pease LR. Clonal evolution in Waldenstrom macroglobulinemia highlights functional role of B-cell receptor. *Blood* 2001; **97**: 321–323.
20 Varettoni M, Zibellini S, Capello D, Arcaini L, Rossi D, Pascutto C *et al.* Clues to pathogenesis of Waldenstrom macroglobulinemia and immunoglobulin M monoclonal gammopathy of undetermined significance provided by analysis of immunoglobulin heavy chain gene rearrangement and clustering of B-cell receptors. *Leuk Lymphoma* 2013; **54**: 2485–2489.
21 Petrikkos L, Kyrtsonis MC, Roumelioti M, Georgiou G, Efthymiou A, Tzenou T *et al.* Clonotypic analysis of immunoglobulin heavy chain sequences in patients with Waldenstrom's macroglobulinemia: correlation with MYD88 L265P somatic mutation status, clinical features, and outcome. *Biomed Res Int* 2014; **2014**: 809103.
22 Kuiatse I, Baladandayuthapani V, Lin HY, Thomas SK, Bjorklund CC, Weber DM *et al.* Targeting the spleen tyrosine kinase with fostamatinib as a strategy against waldenstrom's macroglobulinemia. *Clin Cancer Res* 2015; **21**: 2538–2545.
23 Yang G, Zhou Y, Liu X, Xu L, Cao Y, Manning RJ *et al.* A mutation in MYD88 (L265P) supports the survival of lymphoplasmacytic cells by activation of Bruton tyrosine kinase in Waldenstrom macroglobulinemia. *Blood* 2013; **122**: 1222–1232.
24 Treon SP, Tripsas CK, Meid K, Warren D, Varma G, Green R *et al.* Ibrutinib in previously treated Waldenstrom's macroglobulinemia. *N Engl J Med* 2015; **372**: 1430–1440.
25 Perez OD, Nolan GP. Simultaneous measurement of multiple active kinase states using polychromatic flow cytometry. *Nat Biotechnol* 2002; **20**: 155–162.
26 Irish JM, Doxie DB. High-dimensional single-cell cancer biology. *Curr Top Microbiol Immunol* 2014; **377**: 1–21.
27 Irish JM, Myklebust JH, Alizadeh AA, Houot R, Sharman JP, Czerwinski DK *et al.* B-cell signaling networks reveal a negative prognostic human lymphoma cell subset that emerges during tumor progression. *Proc Natl Acad Sci USA* 2010; **107**: 12747–12754.
28 Palomba ML, Piersanti K, Ziegler CG, Decker H, Cotari JW, Bantilan K *et al.* Multidimensional single-cell analysis of BCR signaling reveals proximal activation defect as a hallmark of chronic lymphocytic leukemia B cells. *PloS One* 2014; **9**: e79987.
29 Xu L, Hunter ZR, Yang G, Zhou Y, Cao Y, Liu X *et al.* MYD88 L265P in Waldenstrom macroglobulinemia, immunoglobulin M monoclonal gammopathy, and other B-cell lymphoproliferative disorders using conventional and quantitative allele-specific polymerase chain reaction. *Blood* 2013; **121**: 2051–2058.
30 Cao Y, Hunter ZR, Liu X, Xu L, Yang G, Chen J *et al.* The WHIM-like CXCR4(S338X) somatic mutation activates AKT and ERK, and promotes resistance to ibrutinib and other agents used in the treatment of Waldenstrom's Macroglobulinemia. *Leukemia* 2015; **29**: 169–176.
31 Jabara HH, McDonald DR, Janssen E, Massaad MJ, Ramesh N, Borzutzky A *et al.* DOCK8 functions as an adaptor that links TLR-MyD88 signaling to B cell activation. *Nat Immunol* 2012; **13**: 612–620.
32 Kurosaki T, Johnson SA, Pao L, Sada K, Yamamura H, Cambier JC. Role of the Syk autophosphorylation site and SH2 domains in B cell antigen receptor signaling. *J Exp Med* 1995; **182**: 1815–1823.
33 Takata M, Kurosaki T. A role for Bruton's tyrosine kinase in B cell antigen receptor-mediated activation of phospholipase C-gamma 2. *J Exp Med* 1996; **184**: 31–40.
34 Ishiai M, Kurosaki M, Pappu R, Okawa K, Ronko I, Fu C *et al.* BLNK required for coupling Syk to PLC gamma 2 and Rac1-JNK in B cells. *Immunity* 1999; **10**: 117–125.
35 Ansell SM, Hodge LS, Secreto FJ, Manske M, Braggio E, Price-Troska T *et al.* Activation of TAK1 by MYD88 L265P drives malignant B-cell Growth in non-Hodgkin lymphoma. *Blood Cancer J* 2014; **4**: e183.
36 Maude SL, Dolai S, Delgado-Martin C, Vincent T, Robbins A, Selvanathan A *et al.* Efficacy of JAK/STAT pathway inhibition in murine xenograft models of early T-cell precursor (ETP) acute lymphoblastic leukemia. *Blood* 2015; **125**: 1759–1767.
37 Sasson SC, Smith S, Seddiki N, Zaunders JJ, Bryant A, Koelsch KK *et al.* IL-7 receptor is expressed on adult pre-B-cell acute lymphoblastic leukemia and other B-cell derived neoplasms and correlates with expression of proliferation and survival markers. *Cytokine* 2010; **50**: 58–68.
38 Krysov S, Potter KN, Mockridge CI, Coelho V, Wheatley I, Packham G *et al.* Surface IgM of CLL cells displays unusual glycans indicative of engagement of antigen in vivo. *Blood* 2010; **115**: 4198–4205.
39 Radcliffe CM, Arnold JN, Suter DM, Wormald MR, Harvey DJ, Royle L *et al.* Human follicular lymphoma cells contain oligomannose glycans in the antigen-binding site of the B-cell receptor. *J Biol Chem* 2007; **282**: 7405–7415.
40 Oka T, Ouchida M, Koyama M, Ogama Y, Takada S, Nakatani Y *et al.* Gene silencing of the tyrosine phosphatase SHP1 gene by aberrant methylation in leukemias/lymphomas. *Cancer Res* 2002; **62**: 6390–6394.
41 Gunawardana J, Chan FC, Telenius A, Woolcock B, Kridel R, Tan KL *et al.* Recurrent somatic mutations of PTPN1 in primary mediastinal B cell lymphoma and Hodgkin lymphoma. *Nat Genet* 2014; **46**: 329–335.
42 Amin R, Mourcin F, Uhel F, Pangault C, Ruminy P, Dupre L *et al.* DC-SIGN-expressing macrophages trigger activation of mannosylated IgM B-cell receptor in follicular lymphoma. *Blood* 2015; **126**: 1911–1920.
43 Castillo JJ, Ghobrial IM, Treon SP. Biology, prognosis, and therapy of waldenstrom macroglobulinemia. *Cancer Treat Res* 2015; **165**: 177–195.
44 Packham G, Krysov S, Allen A, Savelyeva N, Steele AJ, Forconi F *et al.* The outcome of B-cell receptor signaling in chronic lymphocytic leukemia: proliferation or anergy. *Haematologica* 2014; **99**: 1138–1148.
45 Hoogeboom R, van Kessel KP, Hochstenbach F, Wormhoudt TA, Reinten RJ, Wagner K *et al.* A mutated B cell chronic lymphocytic leukemia subset that recognizes and responds to fungi. *J Exp Med* 2013; **210**: 59–70.
46 Quinn ER, Chan CH, Hadlock KG, Foung SK, Flint M, Levy S. The B-cell receptor of a hepatitis C virus (HCV)-associated non-Hodgkin lymphoma binds the viral E2 envelope protein, implicating HCV in lymphomagenesis. *Blood* 2001; **98**: 3745–3749.
47 Parsonnet J, Hansen S, Rodriguez L, Gelb AB, Warnke RA, Jellum E *et al.* Helicobacter pylori infection and gastric lymphoma. *N Engl J Med* 1994; **330**: 1267–1271.

Supplementary Information accompanies this paper on the *Leukemia* website (http://www.nature.com/leu)